Radiation Measurements 176 (2024) 107220

Contents lists available at ScienceDirect

Radiation Measurements

journal homepage: www.elsevier.com/locate/radmeas

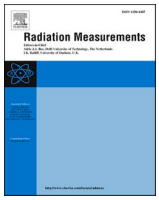

Solid state microdosimetry of a 148 MeV proton spread-out Bragg peak with a pixelated silicon telescope

D. Bortot [a,b,*], D. Mazzucconi [a,b], A. Pola [a,b], S. Agosteo [a,b]

[a] Politecnico di Milano, Milano, Italy
[b] INFN-sezione di Milano, Milano, Italy

ARTICLE INFO

Keywords:
Microdosimetry
Proton therapy
Silicon telescope
Extrapolation algorithm
Proton RBE

ABSTRACT

A constant value of the Relative Biological Effectiveness (*RBE*), equal to 1.1, to weight the physical dose of proton therapy treatment planning collides with the experimental evidence of an increase of effectiveness along the depth dose profile, especially at the end of the particle range. In this context, it is desirable to develop new optimized treatment planning systems that account for a variable RBE when weighting the physical dose. In particular, due to the increasing interest on microdosimetry as a possible methodology for measuring physical quantities correlated with the biological effectiveness of the therapeutic beam, the development of new Tissue-Equivalent Proportional Counters (TEPCs) specifically designed for the clinical environment are in progress.

In this framework, the silicon technology allows to produce solid state detectors of real micrometric dimensions. This is a valid alternative to the TEPC from a practical point of view, being simple, easy-of-use and more versatile. The feasibility of a solid state microdosimeter based on a monolithic double stage silicon telescope has been previously proposed and deeply investigated by comparing its response to the one obtained by reference TEPCs in various radiation fields. The device is constituted by a matrix of cylindrical elements, 2 μm in thickness and 9 μm in diameter, coupled to a single E stage, 500 μm in thickness. Each segmented ΔE stage acts as a solid state microdosimeter, while the E stage gives information on the energy of the impinging proton up to about 8 MeV.

This work is dedicated to the description of the microdosimetric characterization of the 148 MeV energy-modulated proton beam at the radiobiological research line of the Trento Proton Therapy Centre by means of a pixelated silicon microdosimeter. All measurements were carried out at different positions across the spread-out Bragg peak (SOBP) and the corresponding microdosimetric distributions were derived by applying a novel extrapolation algorithm. Finally, microdosimetric assessment of Relative Biological Effectiveness was carried out by weighting the dose distribution of the lineal energy with the Loncol's biological weighting function. Benefits and possible limitations of this approach are discussed.

1. Introduction

A constant value of the Relative Biological Effectiveness (*RBE*), equal to 1.1, for weighting the physical dose of proton therapy treatment planning, collides with the experimental evidence of an increase of effectiveness along the depth dose profile, in particular in its distal fall-off (Paganetti, 2014). The underestimation of the *RBE* in this region of the proton spread-out Bragg peak (SOBP) may result in an excessive dose to healthy tissues downstream of the tumor area: this could lead to an increased toxicity during treatment.

In this framework, new optimized treatment planning systems that consider a variable *RBE* to weight the physical dose are being studied (Willers et al., 2018). Radiobiological assays are commonly employed to evaluate variations of the *RBE* throughout the depth dose profile. Nevertheless, these measurements are time-intensive and entail significant costs, because of the associated complex procedures and protocols. As a valuable alternative, physical quantities that exhibit correlation with biological effectiveness can be measured. It is recognized that an accurate study should require a detailed physical knowledge of the local energy deposition of the therapeutic beam and therefore an accurate beam quality assessment (Wambersie et al., 1990). In particular, due to the increasing interest on microdosimetry as a possible methodology for

* Corresponding author. Politecnico di Milano, Milano, Italy.
E-mail address: davide.bortot@polimi.it (D. Bortot).

https://doi.org/10.1016/j.radmeas.2024.107220
Received 25 January 2024; Received in revised form 26 June 2024; Accepted 28 June 2024
Available online 28 June 2024

measuring physical quantities correlated with the biological effectiveness of the therapeutic beam, the development of new Tissue-Equivalent Proportional Counters (TEPCs) specifically designed for the clinical environment is in progress (Conte et al., 2019).

In this context, the silicon technology allows to produce solid state detectors of real micrometric dimensions. The feasibility of a solid state microdosimeter based on a monolithic double-stage silicon telescope has been previously proposed and deeply investigated by comparing its response to the one obtained by reference TEPCs in various radiation fields (Agosteo et al., 2010, 2011; Colautti et al., 2018; Bianchi et al., 2020). The results show that the microdosimetric spectra measured by the silicon telescope agree satisfactorily with those of a reference TEPC exposed to the same irradiation field when different chord length distributions and materials of the two detectors are considered. This detector is a valid alternative to the TEPC from a practical point of view, being simple, easy-of-use and more versatile. It is a promising device for enhancing the quality assurance of a radio-therapeutic treatment since it does not require any gas system neither high voltage supply.

This work is dedicated to the description of the microdosimetric characterization of the 148 MeV energy-modulated proton beam at the radiobiological research line of the Trento Proton Therapy Centre with a pixelated silicon microdosimeter. Measurements were carried out at different positions across the spread-out Bragg peak. Raw data were elaborated by applying a novel extrapolation algorithm in order to assess the microdosimetric distributions of the lineal energy. Afterwards, microdosimetric assessment of Relative Biological Effectiveness ($RBE\mu$) was carried out by weighting the dose distribution of the lineal energy with the Loncol's biological weighting function (Loncol et al., 1994). A comparison with $RBE\mu$ assessment in the same experimental set-up with a miniaturized Tissue-Equivalent Proportional Counter (mini-TEPC) and a FWT LET-1/2 TEPC (Bianchi et al., 2023) is described and discussed.

2. Materials and methods

2.1. The research beam line of the Trento Proton Therapy Centre

The Trento Proton Therapy Center is a cyclotron based proton therapy center located in Trento (Italy) where proton beams with energies from 70 MeV up to 228 MeV are used for cancer treatment. The facility features two patient rooms, both equipped with 360° rotating gantries, and a unique experimental room provided with two beam lines used exclusively for non-clinical research. The two non-clinical beamlines are used for a variety of physics, radiobiological or biological experiments and they can provide proton beams with a particle rate between 200 and 10^{10} particles per second.

The measurement campaign has been carried out at the facility dedicated to radiobiology research, where a proton beam can be extracted from a cyclotron in the energy range between 70 and 228 MeV. Starting from a fixed pencil beam at 148 MeV, the research beam line is based on a passive scattering system constituted by a first scattering foil followed by a dual-ring system to produce an irradiation field about 6 cm wide with a flat profile at the target position. The energy-depth modulation is obtained with a custom-made range modulator optimized to generate a 2.5 cm spread-out Bragg peak. More details about this research beam line can be found in literature (Tommasino et al., 2019).

2.2. The pixelated silicon microdosimeter

The segmented silicon telescope is a pixelated detector consisting of a matrix of more than 1800 cylindrical ΔE elements coupled to a single residual-energy E stage (500 μm in thickness). Each ΔE element is approximately 1.9 μm thick and of 9 μm in diameter (Agosteo et al., 2008).

Both the ΔE and E stages are fabricated on a single silicon substrate by implanting deeply a p + cathode. Each ΔE element is encircled by a guard ring 14 μm in diameter. This guard ring confines the charge collection within the lateral surface of the sensitive volume (Pola et al., 2020). The pitch between adjacent ΔE elements is about 41 μm. The active areas of the ΔE and E stages are about 0.125 mm^2 and 1 mm^2, respectively.

Both the ΔE and the E stages are biased, and their respective signals are amplified and shaped through two independent electronic chains. Each ΔE pixel acts as a solid state microdosimeter, while the E stage provides information about the energy of the impinging particle. The telescope, moreover, enables discrimination of the type of impinging particle through a scatter-plot.

The tissue-equivalence correction of the energy imparted in the ΔE elements is essential for achieving a microdosimetric spectrum comparable to that obtained with a TEPC. The choice of a telescope detector, as opposed to a single stage, is justified by the significant role played by the E stage in accurately assessing the full energy of impinging protons. The correction procedure involves scaling the energy imparted in a tissue-equivalent ΔE element on an event-by-event basis. Specifically, the energy imparted measured by the silicon ΔE detector is adjusted basing on the ratio of the stopping powers in tissue to that in silicon for a given particle. This correction procedure is effective as long as the primary particle stops completely in the E stage (up to 8 MeV for protons) or in the ΔE stage only. For higher energies, where the ratio of stopping powers in tissue and silicon is fairly constant, an average correction factor is applied. This ensures the accuracy of the microdosimetric spectrum across a broader range of particle energies, thereby enhancing the reliability of the measurements (Agosteo et al., 2010).

Table 1
Thickness of the solid water layers and of the PMMA layers and corresponding water-equivalent depths.

Solid water layer (RW3) [cm]	PMMA layer [cm]	W-E depth [cm]
0.0	0.75	0.88
10.0	0.75	11.20
12.0	0.75	13.26
12.3	0.75	13.57
12.5	0.75	13.78
12.6	0.75	13.88
12.7	0.75	13.99
12.8	0.75	14.09
12.8	0.80	14.15
12.8	0.85	14.21
13.0	0.75	14.30

Fig. 1. Picture of the experimental set-up. From the right to the left the following components are shown: beam pipe, scattering foil, monitor chamber, dual-ring system and range modulator (red square), solid water layers (blue square), silicon telescope (green square).

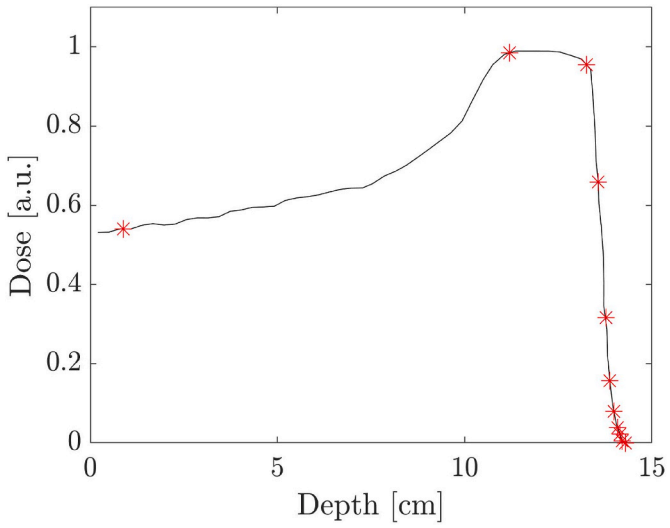

Fig. 2. Depth dose profile and measurement positions of the silicon telescope.

2.3. Experimental set-up

The sensitive volume of the silicon telescope was aligned with the centre of the proton beam and the distance between the microdosimeter and the first scattering foil was maintained equal to 1 m. The silicon telescope was shielded with a 10 μm-thick aluminized Mylar layer. The water-equivalent (W-E) depths across the spread-out Bragg peak were determined by placing a stack of solid water layers (RW3, mass density 1.032 g cm^{-3}) of varying thicknesses between the range modulator and the detector. In order to characterize the microdosimetric distributions at depths as similar as possible to those adopted by Bianchi et al. (2023), a further PMMA (PolyMethylMethAcrylate) layer of 7.5 mm was added to the RW3 stack. It should be noted that this additional layer (equivalent to 8.8 mm in water) does not precisely match the water-equivalent thickness of the mini-TEPC wall, which is 7.9 mm. Additionally, two more depths were obtained by adding an extra PMMA layer of 0.5 mm and 1 mm to the 12.8 cm RW3 layer. Table 1 presents all the combinations of layers utilized to achieve the actual water-equivalent depths. Fig. 1 shows a picture of the experimental set-up, while Fig. 2 reports the depth dose profile with the indication of the measurement positions.

As already mentioned, the ΔE and the E stages of the silicon microdosimeter were biased and their signals were amplified and shaped through two independent electronic chains, with a shaping time of 2 μs for the ΔE and 500 ns for the E. Signals were acquired by a two-channel ADC in coincidence mode to keep the time correlation between the E and ΔE events.

The proton beam current was adjusted to maintain a counting rate of approximately 200 cps for all measurements. The total number of events collected at each measurement position is approximately 10^5.

2.4. Data processing and elaboration

In order to compare the microdosimetric distributions from the two detectors, the energy imparted in the ΔE stage of the silicon telescope $\varepsilon_{\Delta E,Silicon}$ was corrected for tissue-equivalence in propane (the TEPC filling gas) and for the geometrical effect due to their different chord length distribution (due to their different shape).

In particular, the event-by-event correction for tissue-equivalence is based on the following relation (Agosteo et al., 2010):

$$\varepsilon_{\Delta E,Tissue} = \varepsilon_{\Delta E,Silicon} \bullet R(E) = \varepsilon_{\Delta E,Silicon} \bullet \frac{S_{Tissue}(E_{tot})}{S_{Silicon}(E_{tot})} \quad (1)$$

where S is the proton stopping power in tissue and in silicon, respectively, and E_{tot} is the kinetic energy of the impinging particle, obtained as:

$$E_{tot} = \Delta E + E \quad (2)$$

The shape correction, which is based on the mean chord length of protons crossing the ΔE cylindrical sensitive volume (parallel to its axis and equal to 1.9 μm) and the mean chord length of a parallel proton beam crossing a cylindrical sensitive volume normal to its axis (equal to $\frac{\pi}{4}$ μm for a right cylinder with a diameter of 1 μm), allows to define the lineal energy y as (Braby et al., 2023):

$$y = \frac{\varepsilon_{\Delta E,Tissue}}{\left(1.9 * \frac{\pi}{4}\right)\mu m} \quad (3)$$

Experimental data are presented as frequency, $f(y)$, and dose, $d(y)$, distributions of lineal energy, where $f(y)dy$ and $d(y)dy$ represent the fraction of events and the fraction of the absorbed dose, respectively, corresponding to events of lineal energy values between y and y + dy.

As reported in the previous works (Agosteo et al., 2010; Colautti et al., 2020; Bianchi et al., 2020) and highlighted by the scatter plot shown in the following section 3, the energy threshold of the ΔE stage results to be equal to about 15 keV, which corresponds to about 8 keV μm^{-1} in lineal energy. This is the main limitation of the silicon telescope system for microdosimetric assessment of proton beams and it is due to the micrometric thickness of the ΔE pixels which corresponds to a high capacitance and to a high electronic noise. This threshold prevents a direct comparison with TEPC spectra, at least in the proximal region of the SOBP, because a non-negligible portion of the proton microdosimetric spectrum is missing. For this reason, microdosimetric distributions measured with the silicon telescope are generally extrapolated down to 0.01 keV μm^{-1} (Bianchi et al., 2020, 2021; Conte et al., 2020).

In this study, a new extrapolation algorithm was implemented to extend the microdosimetric distribution down to low lineal energies aiming to improve agreement with TEPC distributions. By conducting a thorough analysis of the functional behavior of the low-energy region in distributions measured with the silicon telescope and other microdosimeters across various particle beams and energies, an extrapolation algorithm based on sums of exponential functions was identified as the best fit for the frequency spectrum. Specifically, a double-exponential best fit was applied to experimental frequency distributions within the imparted energy range of 15 keV–25 keV, expressed as:

$$f(\varepsilon) = C_1 e^{k_1 \varepsilon} + C_2 e^{k_2 \varepsilon}$$

where coefficients C_1, C_2, k_1 and k_2 are determined through an unconstrained fit procedure.

This algorithm extrapolated the raw frequency spectrum of the counts from 15 keV (acquisition threshold) down to approximately 0.02 keV without any a-priori information.

To highlight potential advantages and limitations of this new approach, the same raw data within the imparted energy interval of 15 keV–25 keV were also extrapolated using a more common linear extrapolation technique, and the resulting microdosimetric spectra were compared.

Furthermore, a comparison of the obtained full spectra with those presented in Bianchi et al. (2023) was conducted for validation. It should be noted that the water-equivalent depths for the silicon telescope and TEPC measurements are not exactly the same. Apart from the 14.21 cm water-equivalent depth, the corresponding other depths differ by 0.1 mm or 0.2 mm in the distal region of the spread-out Bragg peak and approximately 0.9 mm in its flat region.

Finally, the dose distributions of the lineal energy, $d(y)$, were used to perform an *RBE* assessment (the so called "microdosimetric *RBE*" or RBE_μ) by referring to the Loncol's weighting function r(y) (Loncol et al., 1994), according to the following equation:

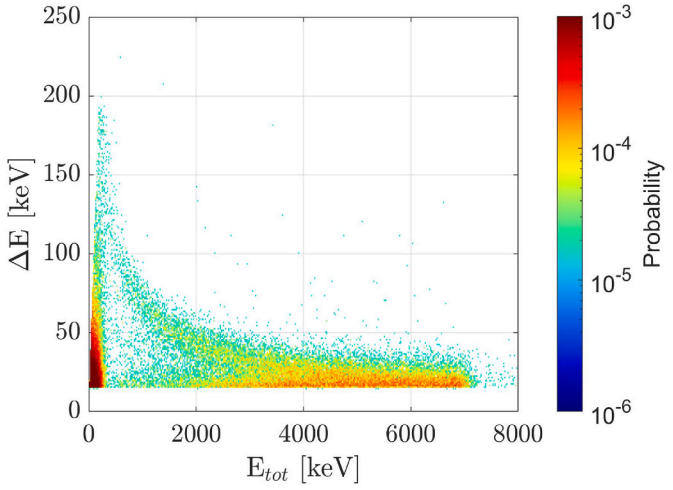

Fig. 3. Scatter-plot (ΔE VS $E_{tot} = \Delta E + E$) measured at 14.09 cm in W-E depth (distal region of the SOBP).

$$RBE_{\mu} = \int r(y)d(y)dy \tag{4}$$

The response function $r(y)$ is determined through a comprehensive correlation of microdosimetric and biological data, establishing a link between the physical characteristics of radiation deposition and its biological impact.

3. Results and discussion

Events from both the ΔE and the E stages of the silicon telescope collected in coincidence mode at 14.09 cm in W-E depth (distal region of the SOBP) are shown, as an example, in the scatter-plot of Fig. 3.

The energy threshold for the ΔE stage, due to the noise level, corresponds to about 15 keV, which is a value consistent with the usual threshold for this microdosimeter (Agosteo et al., 2010). The raw spectra of ΔE signals were then extrapolated as described in section 2.4 down to about 0.02 keV, with no a priori-information about the portion of the spectrum not directly measurable by the silicon microdosimeter. The main purpose of this approach was to investigate the effect of this kind of extrapolation procedure and its robustness for the assessment of the microdosimetric RBE_{μ}.

Moreover, it should be stressed that the telescope detector is crucial for applying the event-by-event tissue-equivalence correction to the ΔE signals based on the actual energy of the impinging particle, according to equation (2). This is particularly true for the distal part of the SOBP, where the adoption of a constant correction factor that approximates the ratio of the stopping power of protons in tissue to that in silicon to a constant value results inadequate, as clearly demonstrated in Agosteo et al. (2010).

After the extrapolation, the tissue-equivalence correction (equation (1)) and the shape correction (equation (3)) have been applied to the data, in order to transform the imparted energy in silicon $\varepsilon_{\Delta E,Si}$ into lineal energy y.

As an example, Fig. 4 shows the dose distribution of lineal energy at 11.20 cm (middle of the SOBP) and 14.09 cm (distal region), obtained before and after the application of the double-exponential extrapolation algorithm to the raw data described above.

It is clear that the threshold remains constant (8 keV μm^{-1}), while the fraction of the absorbed dose directly measurable with the silicon telescope increases for more distal positions, because of the slowing-down of the proton beam which provides an increase of the LET and the shift of the microdosimetric distribution towards high lineal energies. In this way, the artificial region estimated by means of the extrapolation procedure contributes progressively less to the total microdosimetric spectrum by moving towards the distal region of the SOBP.

To underline the advantage of employing a double-exponential extrapolation technique over the typical linear fit, the comparison of silicon microdosimetric distributions assessed through the two different procedures is plotted in Fig. 5 for different water-equivalent depths. Furthermore, the same figure illustrates a further comparison of these spectra with those presented in Bianchi et al. (2023).

This dual comparison clearly demonstrates the superiority of the new algorithm over linear extrapolation: for each water-equivalent depth, the double-exponential extrapolation algorithm yields microdosimetric distributions more closely resembling those measured with the mini-TEPC. In the central region of the proton SOBP, a significant discrepancy between silicon telescope and mini-TEPC data is observed, which is not fully explained by the different depths (11.20 cm versus 11.11 cm and 13.26 cm versus 13.18 cm, respectively). This is attributed to the inability of even the double-exponential extrapolation to fully compensate for the lack of data below the acquisition threshold. However, for more distal positions, the agreement between the spectra becomes increasingly consistent, culminating at the 14.21 cm position, where the two distributions overlap.

It should be underlined that the Loncol's weighting function $r(y)$ is almost constant and equal to 1 below 10 keV μm^{-1} (Loncol et al., 1994), which is a value close to the silicon threshold, therefore it has almost no effect when applied to the $d(y)$ distribution while estimating the microdosimetric RBE_{μ} (Conte et al., 2020). Despite the fact that the dose distributions of lineal energy measured with the silicon telescope and the mini-TEPC are not the same, it is fundamental, at this point of the data elaboration, to investigate the impact of the lack of information in the low lineal energy region (below 8 keV μm^{-1}) to the assessment of the microdosimetric RBE_{μ}.

Fig. 6 shows, as an example, the dose $yd(y)$ and the biological-

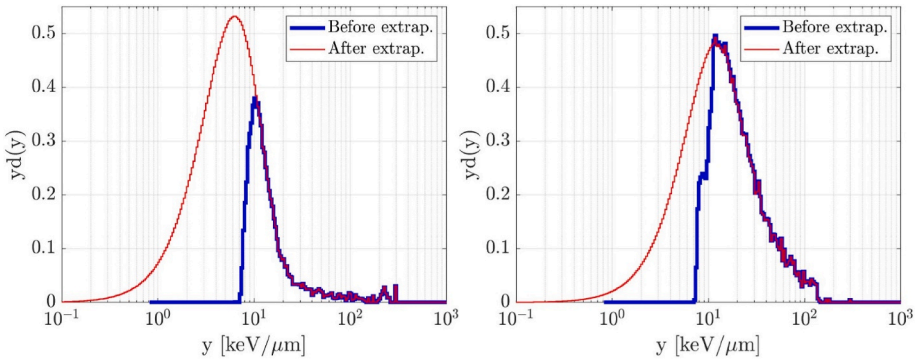

Fig. 4. Microdosimetric distributions at 11.20 cm (flat region of the SOBP) and 14.09 cm (distal region of the SOBP) before and after the application of the double-exponential extrapolation algorithm to the raw data described in the text.

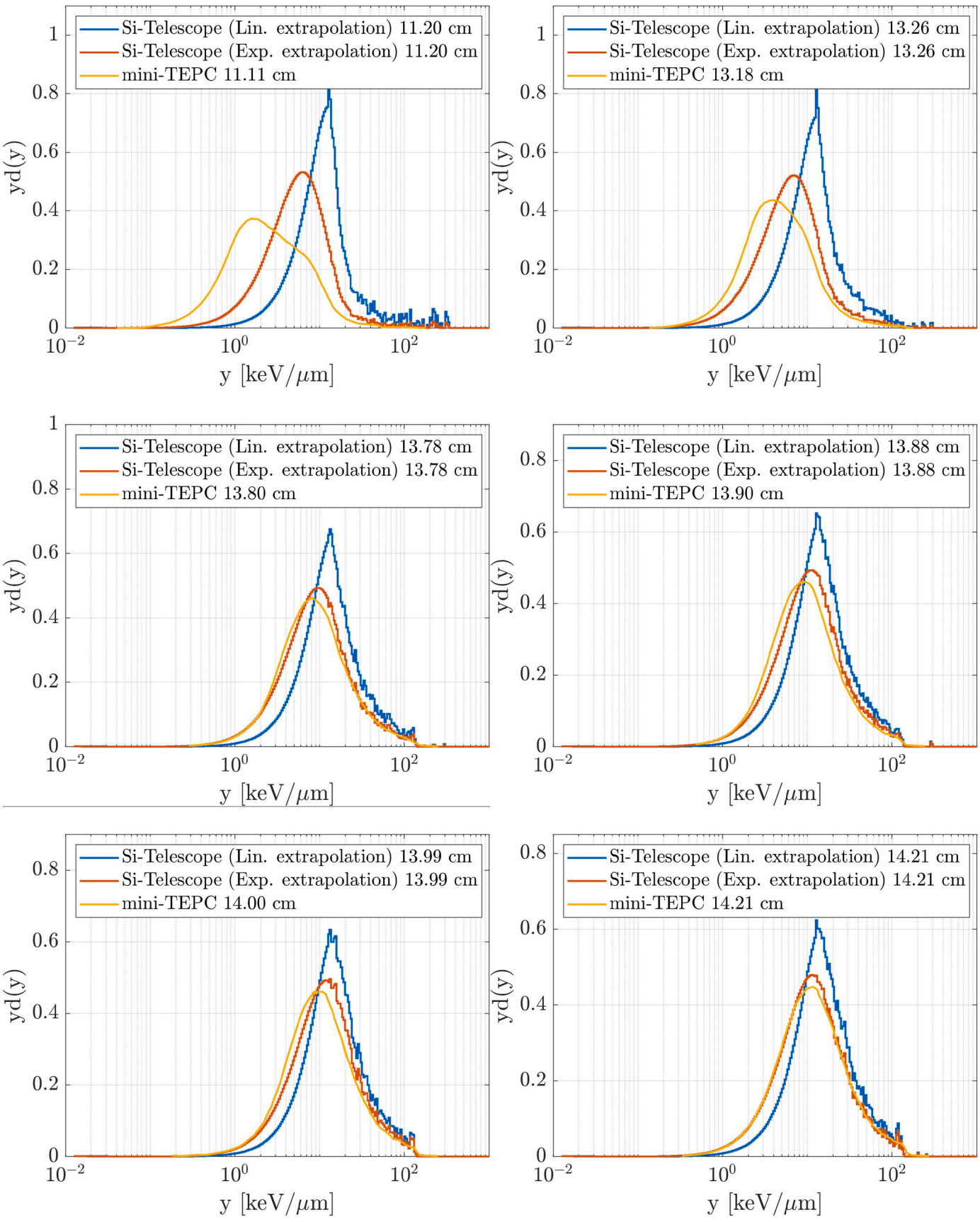

Fig. 5. Microdosimetric distributions at different water-equivalent depths obtained with a linear (blue line) and a double-exponential (orange line) extrapolation algorithm. The microdosimetric spectra measured with the mini-TEPC (Bianchi et al., 2023) at the corresponding depth are included for reference (yellow line).

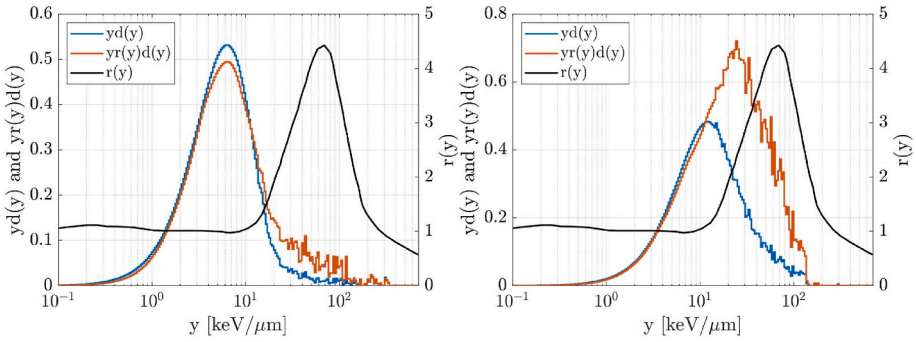

Fig. 6. Dose distribution $yd(y)$ and biological-weighted distribution $yr(y)d(y)$ at 11.20 cm and 14.09 cm in W-E depth, together with the Loncol's function $r(y)$.

Table 2
Microdosimetric RBE_μ assessed via equation (4) as a function of the water-equivalent depth and comparison with the values reported in Bianchi et al. (2023).

	RBE_μ	
W-E depth [cm]	Silicon telescope (this work)	Mini-TEPC (Bianchi et al., 2023)
0.79	–	1.03 ± 0.03
0.88	1.01 ± 0.05	–
11.11	–	1.03 ± 0.03
11.20	1.05 ± 0.04	–
13.18	–	1.10 ± 0.03
13.26	1.12 ± 0.03	–
13.49	–	1.23 ± 0.04
13.57	1.24 ± 0.04	–
13.69	–	1.31 ± 0.04
13.78	1.36 ± 0.04	–
13.80		1.38 ± 0.04
13.88	1.46 ± 0.04	–
13.90	–	1.42 ± 0.04
13.99	1.52 ± 0.05	–
14.00	–	1.48 ± 0.04
14.09	1.56 ± 0.05	–
14.15	1.58 ± 0.05	–
14.21	1.52 ± 0.05	1.57 ± 0.05
14.30	1.44 ± 0.04	–

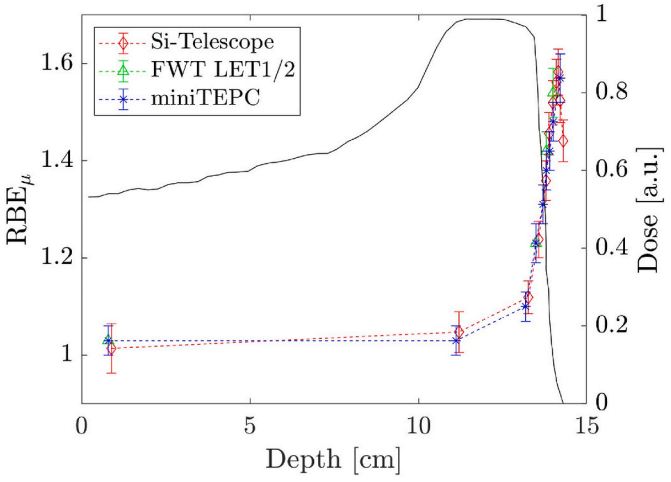

Fig. 7. Microdosimetric RBE_μ obtained via equation (4) as a function of the water-equivalent depth: comparison between silicon telescope (this work) and two different reference TEPCs (i.e. FWT LET-1/2 TEPC and mini-TEPC) for the same experimental set-up (Bianchi et al., 2023).

weighted distributions $yr(y)d(y)$ at 11.20 cm and 14.09 cm in W-E depth. Both distributions were multiplied by y, so that equal area under each curve between two values of y correspond to equal relative contributions to the absorbed dose and to the RBE_μ, respectively. Note that $d(y)$ is the normalized dose distribution, while the integral of $r(y)d(y)$ over the whole y-range, proportional to the area subtended by the $yr(y)d(y)$ curve, is the microdosimetric RBE_μ, according to equation (4). The Loncol's function $r(y)$ is also reported as a reference.

It should be noted that the $yd(y)$ and the weighted $yr(y)d(y)$ spectra are very similar to each other, when the main part of the $yd(y)$ spectrum falls below y = 10 keV μm^{-1}, because the $r(y)$ function is almost constant and equal to one. Consequently, the integral of the weighted distribution is close to the integral of the $d(y)$ distribution, which is equal to 1 by definition.

When the spectral component above y = 10 keV μm^{-1} increases, in the region where the $r(y)$ function also increases, the effect of the weighting function appears and become stronger as the $yd(y)$ spectrum shifts to the right, in the region between 10 and 100 keV μm^{-1}. The strongest increment is for events with lineal energy y ∼ 70 keV μm^{-1}, where the Loncol's function r(y) is at its maximum. Eventually, above 200 keV μm^{-1}, the $r(y)$ function drops to values lower than 1, causing a decrease in RBE_μ.

The whole set of RBE_μ values obtained via equation (4) as a function of the water-equivalent depth is listed in Table 2, together with the corresponding values measured by Bianchi et al. (2023). The same data are shown in Fig. 7, where the depth dose profile is also indicated. The uncertainty is based on the statistical uncertainty in the number of counts in the frequency spectrum.

The results are in very good agreement. The RBE_μ is about 1 at the entrance, increases up to 1.25 in the SOBP, and reaches values of about 1.58 in the distal fall-off. At the last measured depth (14.30 cm), the silicon microdosimeter allowed to appreciate a decrease in RBE_μ with respect to the maximum value, down to 1.44. This decrease is due to the fact that this depth is beyond the Bragg peak, where the measured microdosimetric distribution is shifted toward lower lineal energy values. This shift may be associated with the recoil ions set in motion by the secondary neutron field produced in the irradiation room.

In general, the mini-TEPC, the FWT LET-1/2" and the silicon telescope data agree within a 5% estimated uncertainty. It should be mentioned that these values are in good agreement with several radiobiological observations (Paganetti, 2014).

4. Conclusions

A microdosimetric characterization of the 148 MeV energy-modulated proton beam at the radiobiological research line of the Trento Proton Therapy Centre has been carried out with a pixelated silicon microdosimeter. Measurements were performed at eleven different depths across the spread-out Bragg peak.

A systematic double-exponential extrapolation algorithm has been applied to the measured data, in order to extend the microdosimetric distribution down to low lineal energies, and both corrections for tissue-equivalence and shape were adopted.

The microdosimetric spectra show an increasing contribution of large size lineal energy events when the depth increases, consistent with the slowing down of the proton beam. The *RBE* estimated through microdosimetric dose distributions weighted with the Loncol's function are in good agreement with literature data. It is therefore confirmed that the RBE_{μ} varies with increasing depth, being about 1 at the entrance, 1.25 in the Bragg peak and 1.58 in the distal fall-off. A decrease down to 1.44 is observed at the last measured depth beyond the Bragg peak.

These results demonstrate that the new extrapolation algorithm applied to measured data, which is based on exponential functions with no further information about the expected distribution, allows to obtain microdosimetric RBE_{μ} values consistent with those measured with reference TEPCs in a modulated 148 MeV proton beam.

A future work will be dedicated to the application of the same procedure for data measured with different therapeutic proton beams in order to confirm its robustness. This approach could be, in principle, a possible alternative for assessing $RBE\mu$ values not only in the distal region of the SOBP, but also in the proximal one.

CRediT authorship contribution statement

D. Bortot: Writing – original draft, Visualization, Validation, Methodology, Investigation, Formal analysis, Conceptualization. **D. Mazzucconi:** Writing – review & editing, Investigation, Formal analysis, Data curation, Conceptualization. **A. Pola:** Supervision, Conceptualization. **S. Agosteo:** Writing – review & editing, Supervision, Project administration, Investigation, Funding acquisition.

Declaration of competing interest

The authors declare that they have no known competing financial interests or personal relationships that could have appeared to influence the work reported in this paper.

Data availability

Data will be made available on request.

Acknowledgements

This work was supported by the 5th Scientific Commission of the Italian Institute for Nuclear Physics (INFN) in the framework of the Microbe_IT experiment. The authors would like to acknowledge Enrico Verroi for its technical support during the measurement campaign.

References

Agosteo, S., Fallica, P.G., Fazzi, A., Introini, M.V., Pola, A., Vulva, G., 2008. A pixelated silicon telescope for solid state microdosimetry. Radiat. Meas. 43, 585–589.
Agosteo, S., Cirrone, G.A.P., Colautti, P., Cuttone, G., D'Angelo, G., Fazzi, A., Introini, M. V., Moro, D., Pola, A., Varoli, V., 2010. Study of a silicon telescope for solid state microdosimetry: preliminary measurements at the therapeutic proton beam line of CATANA. Radiat. Meas. 45, 1284–1289.
Agosteo, S., Colautti, P., Fanton, I., Fazzi, A., Introini, M.V., Moro, D., Pola, A., Varoli, V., 2011. Study of a solid state microdosimeter based on a monolithic silicon telescope: irradiations with low-energy neutrons and direct comparison with a cylindrical TEPC. Radiat. Protect. Dosim. 143, 432–435.
Bianchi, A., Selva, A., Colautti, P., Bortot, D., Mazzucconi, D., Pola, A., Agosteo, S., Petringa, G., Cirrone, G.A.P., Reniers, B., Parisi, A., Struelens, L., Vanhavere, F., Conte, V., 2020. Microdosimetry with a sealed mini-TEPC and a silicon telescope at a clinical proton SOBP of CATANA. Radiat. Phys. Chem. 171, 108730.
Bianchi, A., Selva, A., Colautti, P., Parisi, A., Vanhavere, F., Reniers, B., Conte, V., 2021. The effect of different lower detection thresholds in microdosimetric spectra and their mean values. Radiat. Meas. 146, 106626.
Bianchi, A., Selva, A., Rossignoli, M., Pasquato, F., Missaggia, M., Scifoni, E., La Tessa, C., Tommasino, F., Conte, V., 2023. Microdosimetry with a mini-TEPC in the spread-out Bragg peak of 148 MeV protons. Radiat. Phys. Chem. 202, 110567.
Braby, L.A., Conte, V., Dingfelder, M., et al., 2023. ICRU report 98. Stochastic nature of radiation interactions: microdosimetry. J. ICRU 23 (1), 1–168.
Colautti, P., Conte, V., Selva, A., Chiriotti, S., Pola, A., Bortot, D., Fazzi, A., Agosteo, S., Ciocca, M., 2018. Microdosimetric study at the CNAO active-scanning carbon-ion beam. Radiat. Protect. Dosim. 180 (1–4), 157–161.
Colautti, P., Bianchi, A., Selva, A., Bortot, D., Mazzucconi, D., Pola, A., Agosteo, S., Petringa, G., Cirrone, G., Conte, V., 2020. Therapeutic proton beams: LET, RBE and microdosimetric spectra with gas and silicon detectors. Radiat. Meas. 136, 106386.
Conte, V., Bianchi, A., Selva, A., Petringa, G., Cirrone, G.A.P., Parisi, A., Vanhavere, F., Colautti, P., 2019. Microdosimetry at the CATANA 62 MeV proton beam with a sealed miniaturized TEPC. Phys. Med. 64, 114–122.
Conte, V., Agosteo, S., Bianchi, A., Bolst, D., Bortot, D., Catalano, R., Cirrone, G.A.P., Colautti, P., Cuttone, G., Guatelli, S., James, B., Mazzucconi, D., Rosenfeld, A.B., Selva, A., Tran, L., Petringa, G., 2020. Microdosimetry of a therapeutic proton beam with a mini-TEPC and a MicroPlus-Bridge detector for RBE assessment. Phys. Med. Biol. 65, 245018.
Loncol, T., Cosgrove, V., Denis, J.M., Gueulette, J., Mazal, A., Menzel, H.G., Pihet, P., Sabattier, R., 1994. Radiobiological effectiveness of radiation beams with broad LET spectra: microdosimetric analysis using biological weighting functions. Radiat. Protect. Dosim. 52, 347–352.
Paganetti, H., 2014. Relative biological effectiveness (RBE) values for proton beam therapy. Variations as a function of biological endpoint, dose, and linear energy transfer. Phys. Med. Biol. 59, R419–R472.
Pola, A., Bortot, D., Mazzucconi, D., Fazzi, A., Galer, S., Kirkby, K.J., Merchant, M.J., Palmans, H., Agosteo, S., 2020. Characterization of a pixelated silicon microdosimeter in micro-beams of light ions. Radiat. Meas. 133, 106296.
Tommasino, F., Rovituso, M., Bortoli, E., La Tessa, C., Petringa, G., Lorentini, S., Verroi, E., Simeonov, Y., Weber, U., Cirrone, P., Schwarz, M., Durante, M., Scifoni, E., 2019. A new facility for proton radiobiology at the Trento proton therapy centre: design and implementation. Phys. Med. 58, 99–106.
Wambersie, A., Pihet, P., Menzel, H.G., 1990. The role of microdosimetry in radiotherapy. Radiat. Protect. Dosim. 31, 421–432.
Willers, H., Allen, A., Grosshans, D., McMahon, S.J., von Neubeck, C., Wiese, C., Vikram, B., 2018. Toward A variable RBE for proton beam therapy. Radiother.Oncol. J. Eur. Soc.Therapeut.Radiol. Oncol. 128 (1), 68–75.